

**The M_V^{HB} vs. $[\text{Fe}/\text{H}]$ Calibration: I.
HST Color-Magnitude Diagrams of
8 Globular Clusters in M 31**

F. Fusi Pecci¹, R. Buonanno², C. Cacciari¹,
C.E. Corsi², S.G. Djorgovski³, L. Federici¹,
F. R. Ferraro¹, G. Parmeggiani¹, R.M. Rich⁴

ABSTRACT

Color Magnitude Diagrams (CMDs) of individual stars in 8 Globular Clusters (GCs) in M31 down to about 1 mag fainter ($V \sim 26.5$) than the Horizontal Branch (HB) have been obtained with the *Hubble Space Telescope -HST*.

In particular, we observed G280 and G351 with the FOC ($f/96 + F430W$ and $f/96 + F480LP$) while the WFPC2 (F555W, F814W) frames for G1, G58, G105, G108, G219+Bo468 were retrieved from the *HST* archive.

The cluster metallicities - $[\text{Fe}/\text{H}]$ - range from -1.8 to -0.4. Coupled with sufficiently accurate (to $\sim \pm 0.1$ mag) measures of the mean brightness of the HB - V_{HB} -, appropriate estimates of reddening for each cluster, and the adoption of a distance modulus to M31 of $(m-M)_o = 24.43$, this has allowed us to yield a direct calibration for the mean absolute magnitude of the HB at the instability strip - M_V^{HB} - with varying $[\text{Fe}/\text{H}]$:

$$M_V^{HB} = (0.13 \pm 0.07) [\text{Fe}/\text{H}] + (0.95 \pm 0.09)$$

where the associated errors result from the adopted global errors in the measure and best fitting procedures.

The slope of the derived relation is fully consistent with that predicted by the standard and canonical models (~ 0.15) and obtained by various ground-based observations, while it is only marginally compatible with higher values (~ 0.30), also obtained in the past.

¹Osservatorio Astronomico di Bologna, Via Zamboni 33, 40126 Bologna, Italy

²Osservatorio Astronomico di Monte Porzio, Roma, Italy

³Division of Physics, Mathematics, and Astronomy, California Institute of Technology, Pasadena, CA 91125, USA

⁴Department of Astronomy, Columbia University, New York, NY 10027, USA

The zero-point, which is crucial to *absolute* age determinations, depends on the adopted distance to M31 and is moreover affected by an additional error due to the residual uncertainties in the *HST* photometric zero-points (~ 0.05 mag, at least).

If confirmed, such a calibration of the M_V^{HB} vs. $[\text{Fe}/\text{H}]$ relationship would imply *old* absolute ages ($> 16\text{Gyr}$) for the oldest Galactic globulars and fairly small age spread among those having a constant magnitude difference between the Main-Sequence Turnoff and the HB.

Subject headings: Clusters: Globular (126); Galaxies: Individual, M31 (140); Distance scale: RR Lyrae variables; Photometry: HST

1. Introduction

Horizontal Branch (HB) stars are fundamental standard candles for Population II systems, and consequently are important tools for deriving ages of globular clusters (GCs) from the Main - Sequence Turnoff (TO) luminosity.

While other techniques exist to calibrate the TO luminosity, they require high photometric precision at faint magnitudes, so the use of the magnitude difference between TO and HB – ΔV_{HB}^{TO} – remains, in our opinion, one of the best approaches to age determination for most of the Galactic GCs. However the conflict between the large ages estimated for globular clusters and the smaller values derived from the expansion models is a source of considerable concern for standard cosmological studies.

The luminosity level of the HB – M_V^{HB} –, namely its absolute “vertical” location in the HR diagram, is expected (based on stellar evolution theory) to depend on metallicity – $[\text{Fe}/\text{H}]$. Despite considerable effort over the last decade, the slope of this relation is still not known very accurately, ranging from ~ 0.15 to ~ 0.37 (see Sandage 1993 for a recent review). The zero point is also uncertain at the 0.25 mag level, and these uncertainties propagate into an error of at least ± 3 Gyr in the determined absolute ages of Galactic GCs. Therefore the current uncertainties are too large and make it impossible to assess if the GGCs have an age-metallicity relation.

The age calibration of the observable parameter ΔV_{HB}^{TO} (Buonanno et al. 1989, Sandage and Cacciari 1990, Walker 1992, Bolte and Hogan 1995, Chaboyer et al. 1996, Buonanno et al. 1996, Catelan & de Freitas Pacheco 1996) critically depends on the M_V^{HB} vs. $[\text{Fe}/\text{H}]$ relation. Since ΔV_{HB}^{TO} has been measured for several GGCs spanning from the outer halo to the Galactic Bulge, a firm knowledge of this relation will have a widespread impact on the age question in general, and on the models of galaxy formation in particular.

By extending to the nearest giant spiral galaxy M31 the same type of studies of the GC family that have become classical for our own Galaxy, it is possible to solve the problem of the precise

measurement of the absolute luminosity of HB stars with varying metallicity, being the clusters in practice at the same distance to us.

The M31 globular cluster system offers a unique opportunity for stellar population studies (see for references Brodie 1993, Fusi Pecci et al. 1993, Huchra 1993). The cluster population is extremely rich, and the proximity of M31 allows the horizontal and giant branch populations to be resolved with *HST*. Most of the bright M31 clusters are not seen projected against a disk population (as is the case for M33). Almost all the clusters appear to be as old as those of the Milky Way halo, with a wide range of metallicities (which represents a significant difference from the case of the Magellanic Clouds). In M31 we have the further advantage that the distance dispersion is at most $\Delta (m-M)_o \sim 0.15\text{mag}$ (corresponding to a maximum intrinsic depth of the M31 GC system of about 100 Kpc) and the reddening distribution is rather uniform, allowing comparative studies that are impossible to undertake for Milky Way clusters.

Beginning with Heasley et al. (1988) and continuing to present samples (Couture et al. 1995) even the best ground-based efforts using CFHT have failed to reach the HB and resulted in photometry of a handful of the brightest and most external stars in each cluster. Hence, *HST* is the only instrument presently capable of carrying on this project.

This program was proposed as a GTO Program (no. 1283; subsequently withdrawn) and approved as GO 5420 in Cycle 4. Data from FOC/96 obtained during Cycle 1 (GO 2583) has resulted in publication of excellent surface brightness profiles for 13 clusters (Fusi Pecci et al. 1994) including the discovery of the first post-core collapse M31 globular cluster, which could not have been discovered from the ground (Bendinelli et al. 1993).

Taking full advantage of the post-refurbishment characteristics, at the end of Cycle 5 a total of 12 M31 clusters will have been observed with WFPC2 or COSTAR+FOC. We present here the CMDs obtained from the reduction and analysis of 8 clusters. Two of them have been observed by us with the FOC, and for the other six we retrieved the available archive WFPC2 data. Table 1 lists the program clusters as identified in the various catalogs (G = Sargent et al. 1977, Bo = Battistini et al. 1993, V = Vetsnik 1962) and a few basic data.

2. Observations and reductions

The full description of the detailed photometric treatments and the data is postponed to a forthcoming paper where also the surface brightness profiles and the structural cluster parameters will be measured and discussed.

2.1. FOC-data

The completely refurbished and properly aligned and focused *HST* +COSTAR system with the high resolution Faint Object Camera (FOC) offers in principle a powerful tool to study the GCs in the distant galaxies of the Local Group. In particular, the M 31 GCs are the ideal targets since at this distance (~ 770 Kpc) the typical dimension of a GC (~ 25 pc) corresponds to only $7''$, and this perfectly fits into the FOC field of view. In addition, the FOC is the *HST* camera with the highest space resolution, which is desirable for the photometry of individual stars and cannot be matched by the space resolution of ground based observations even in excellent seeing conditions.

The data presented here were obtained on 18-19 January 1995 and 23 January 1995, for the M31 GCs G351 and G280, respectively, using the 512×512 pixel² imaging mode of the f/96 camera of the COSTAR-corrected FOC. In this configuration the pixel size is $0''.0144 \times 0''.0144$ and the field of view is $\sim 7'' \times 7''$ (Jedrzejewski et al. 1994). Five exposures ($4 \times 2300 + 1 \times 1600$ sec) were obtained using the F480LP filter and two ($1500 + 2300$ sec) using the F430W on each cluster.

The raw images were flattened and geometrically corrected using the standard STScI pipeline calibration procedure in order to remove the optical distortions.

All images in each filter have been registered and co-added in order to increase the S/N of the faint stars. The final images ready for reduction correspond to an effective exposure time of 10,783 sec and 3793.2 sec in the F480LP and F430W filter, respectively. Figure 1 presents the result of this procedure for G351 (F480LP).

The standard searching procedure available in ROMAFOT (see Ferraro *et al.* 1991) was then applied to each frame, excluding a small central area (with $r < 130$ and $r < 150$ pixels corresponding to 1.9 and 2.2 arcsec for G351 and G280, respectively) in order to avoid regions which are too severely crowded even with *HST*. More than 800 objects have been identified in each cluster in the (deepest) F480LP frames, and these identifications were subsequently used as input for the fitting procedure also in the F430W frames. An interactive check of all the objects was carried out in the F430W frames over a wide annulus to increase the degree of completeness of at least the brightest sample.

The photometry of individual stars on the co-added frames was performed using ROMAFOT (Buonanno et al. 1983), purposely adapted to handle *HST* data. In particular, the *HST* point spread function (PSF) has been modelled by a Moffat (1969) function in the central part of the profile plus a numerical experimental map of the residuals in the wings. The optimal PSF has been determined from the analysis of the brightest uncrowded stars independently in both co-added frames.

The instrumental magnitudes resulting from the PSF fitting procedure have been transformed to the *HST* photometric system by using a sample of selected isolated stars whose magnitudes have been computed using both the fitting procedure and the classic aperture photometry. For

these reference stars *HST* magnitudes have been computed using the formula (HST Handbook Data p.116, and Nota 1995, private communication):

$$Mag_{HST} = -21.10 - 2.5 \text{Log}((c \times U)/(\epsilon \times t))$$

where c represents the stellar counts, U is the inverse sensitivity function, t is the exposure time in sec, and ϵ is the fraction of the encircled energy within the area considered.

On the basis of the values of the encircled energy within 2 pixels (radius) reported in Table 8 of the FOC Handbook (Version 5.0, May 1994), we adopted $\epsilon_{F430W} = 0.46$ and $\epsilon_{F480LP} = 0.42$. For the inverse sensitivity function we have used $U_{F430W} = 0.28129 \times 10^{-17}$ and $U_{F480LP} = 0.57939 \times 10^{-17} \text{ erg cm}^{-2} \text{ A}^{-1}$.

To construct an empirical transformation from the *HST* magnitude system to the Johnson standard system, we have chosen a set of (V,B-V) points appropriate to define the fiducial Red Giant Branch (RGB) and HB for a wide sample of Galactic GCs. To each (V,B-V) pair we have then associated a simulated stellar spectrum of appropriate luminosity and spectral type generated from the Kurucz (1979) stellar atmosphere models. Finally, by running FOCSIM (W.J.Hack, The FOCSIM Beginners Manual, Version 2.0, May 1993) we have obtained the following transformations:

$$B = m_{F430W}^0 - 0.43 \times (m_{F430W} - m_{F480LP})^0 + 0.51$$

$$V = m_{F480LP}^0 - 0.20 \times (m_{F430W} - m_{F480LP})^0 + 0.04$$

where $(m_{F430W} - m_{F480LP})^0$ is the dereddened color in the *HST* system, and m_{F430W}^0 and m_{F480LP}^0 are the dereddened *HST* magnitudes computed by adopting $A_{F480LP} = 3.46 \times E(B - V)$ and $A_{F430W} = 4.47 \times E(B - V)$ (Savage and Mathis 1979). The calibration curves in each color are plotted in Figure 2a,b. This procedure assumes that the reddening $E(B-V)$ is known. See Sect. 3.3 for a description of our reddening assumptions.

2.2. WFPC2-data

The images used in the present study have been retrieved from the *HST* archive. They consist of the data obtained in February 1994 (prior to the cooldown of the WFPC2) on G58, G105, G108 and G219 with the GTO program 5112 (P.I.: J. Westphal) and those obtained on G1 as a part of Cycle 4 program GO 5464 (P.I.: M. Rich) in July 1994 (after the cooldown). In addition, we have reduced and analysed also the small globular cluster Bo468 which fell in the WF3 frame of the exposures taken primarily for G219. The results obtained from this material have been published by Ajhar et al. (1996) and Rich et al. (1995), respectively, except for Bo468 which has never been studied before.

Although the CMDs presented by these two groups are of excellent quality, we believed that a new independent analysis of the whole data set was worth the effort, in order to combine all the

available information on the *HST* CMDs of M31 GCs in the most homogeneous way as possible. Of course, we have the problem of comparing data from two different instruments, with the additional complication that some WFPC2 data were taken before and some after the camera was cooled down from -77 to -88°C. Nevertheless, the use of the same reduction procedure will at least minimize the differences in the photometric treatments, and we believe we have taken as much care as possible to account for the intrinsic and systematic differences between the instruments.

In particular, we have reduced all the PC frames taken from GTO 5112 (2×1000s with F555W (V) + 2×1000s with F814W (I)) and the related WF3 frames which contained Bo468, and the PC frames taken with the same filters from GO 5464 (1600s with F555W (V) + 1200s with F814W (I), in total). Concerning the pre-processing and calibrating procedures, since we have simply retrieved the data from the *HST* Archive, we have strictly adopted the pipeline applied at the STScI.

The analysis of the available frames has been carried out following two main methods, *i.e.* by cosmic-ray cleaning and co-adding the frames to yield a master image in each color on which the photometric measurements were performed, or by independently reducing and measuring all the frames and subsequently matching and averaging the individual sets to yield a final cross-checked sample. To our experience, the first method yields slightly deeper samples (by about half a magnitude), whilst the second yields a better photometric accuracy for the objects down to about one magnitude above the frame limit.

As reported above for the FOC data, the study of the PSF, the search for the objects, and the measure of the instrumental magnitudes have been carried out by using ROMAFOT (Buonanno et al. 1983), excluding a small central area (with $r < 30$ pixels corresponding to ~ 1.5 arcsec for G58, $r < 45$ pixels corresponding to ~ 2 arcsec for G105, G108, G219, and $r < 15$ pixels corresponding to ~ 1.5 arcsec for Bo468) in order to avoid regions where the crowding is too severe even with *HST*. About 1987, 1216, 555, 1228 (+ 1466 in the field), 726 and 335 (+ 1580 in the field) stellar objects have been identified in G1, G58, G105, G108, G219 and Bo468 respectively, in the (deepest) F814W frames. These identifications were subsequently used as input for the fitting procedure also in the F555W frames.

The instrumental magnitudes resulting from the fitting procedure have been transformed to the *HST* photometric system by using a sample of selected isolated stars whose magnitudes have also been computed using the classic aperture photometry after correcting for CTE effects (Holtzman et al. 1995). For these reference stars *HST* magnitudes have been computed using the formula (Holtzman et al. 1995):

$$V = F555W - 0.052(V - I)_0 + 0.027(V - I)_0^2 + 21.725 + 2.5\log_{10}(1.987)$$

$$I = F814W - 0.062(V - I)_0 + 0.025(V - I)_0^2 + 20.839 + 2.5\log_{10}(1.987) + c$$

where c has been set equal to +0.05 for the observations taken from GTO 5112 (with the detector operating at -77°C) and equal to 0.00 for G1 (from GO 5464, at -88°C) as done by Ajhar et al. (1996) and Rich et al. (1995), respectively.

2.3. Photometric errors and comparison with previous photometries

Both Ajhar et al. (1996) and Rich et al. (1995) have widely discussed the problem of estimating the global (*i.e.* internal + systematic) errors in the *HST* photometry of the M31 GCs, also using simulations and artificial star experiments. A detailed discussion of our photometric errors and a complete comparison with the previous photometries will be presented in the forthcoming full paper. We report here schematically the main conclusions and figures.

The *internal* errors are mostly due to noise from the sky, imperfections of the PSF fitting, and blending effects. The method adopted with ROMAFOT to describe the PSF is particularly effective in reducing the size of the internal errors essentially because of the combination of a "known" Moffat-function and a map of the local residual plus a multicomponent fitting procedure. A rough quantitative estimate of the internal errors can be obtained by computing the r.m.s. scatter of the individual measures for the same stars on different frames. Adopting the formula taken from Ferraro et al. (1991) one has $\sigma_V \sim 0.02$ mag and $\sigma_I \sim 0.02$ mag in the interval $22 < V < 24$ and $\sigma_V \sim 0.05$ mag and $\sigma_I \sim 0.06$ mag in the interval $24 < V < 27$.

Another straightforward way of estimating our internal errors can be the direct comparison of the observed widths of the various branches in the final CMDs for the clusters in common with previous studies based on the same original *HST* data. Figure 3a,b compares the CMDs of G 105 as obtained here and as reported in Figure 9 of Ajhar et al. (1996). As one can see, both the location and the spread of the points around the main ridge lines are comparable, and even the substructures along the branches are very similar. This ensures that the photometric quality of the reductions are comparable, and we conclude that our *internal* photometric errors are not larger than those quoted by Ajhar et al. (1996), which they claimed to be fully consistent with those expected from their simulations.

Concerning the *systematic* errors, there are many reasons of uncertainty and most of them can hardly be quantified safely. In particular, there are problems related to charge transfer efficiency (CTE) with WFPC2. Then, there are uncertainties in the conversion to Standard System for both cameras. Finally, there is additional concern about the exact zero-points of the HST photometric systems.

We do not have any special information and new data on these items and refer to the thorough discussions reported for the two cameras by Holtzman *et al.* (1995), Ajhar et al. (1996), Cool and King (1995), Rich et al. (1995).

In conclusion, we believe that while the *internal errors* are as close as possible to the minimum limit achievable, the residual *systematic* errors, especially in the zero-points, can still be quite large (up to 0.05 mag, Ajhar et al. (1996)). This may have a strong impact on the following discussion as we are forced to combine data taken from different cameras, and from the same instrument operated at different temperature conditions. Since the whole problem of absolute calibrations (both with FOC and WFPC2) is under investigation, it is natural to conclude that any differential

variation of the zero-points for one of the used configurations will affect the final results.

3. The data

3.1. The Color Magnitude Diagrams

The CMDs eventually obtained from all the measured stars in the 8 clusters are reported in Figure 4*a – h*. The clusters are shown in order of increasing metallicity (see Table 3, col. 4) to put into evidence the regular trend in the variation of the CMD morphology with varying $[\text{Fe}/\text{H}]$. In fact, as one can easily see from Figure 4, the slope of the giant branch decreases progressively while the HB runs from the blue for G 219 –the most metal-poor cluster– to the red for G 280 –a cluster with almost solar $[\text{Fe}/\text{H}]$.

As already pointed out by Ajhar et al. (1996) and Rich et al. (1995), this overall behaviour makes the CMDs of the observed M31 GCs essentially identical to those of Galactic globulars having the same $[\text{Fe}/\text{H}]$. In particular, it is remarkable to note the increasing bending of the bright giant branch with increasing metallicity, which leads the most metal rich objects to display the well-known turn-over towards very red colors (Ortolani et al. 1990, Bica et al. 1991, Ortolani et al. 1992).

Since our specific aim here is to determine the M_V^{HB} vs. $[\text{Fe}/\text{H}]$ relation, we postpone any further quantitative analysis and discussion of the CMDs, and simply report the procedure followed to derive the quantities involved in this calibration.

3.2. The cluster ridge lines

To properly define meaningful ridge lines one must clean the cluster sample from contaminating objects and select a sub-sample of stars measured in annular regions appropriate to optimize the stellar statistics with respect to the photometric quality (i.e. maximum number of stars with minimum blending and crowding problems).

We have therefore plotted radial CMDs over various (4-6) annuli centered on each cluster and selected the best region to trace the ridge lines of the various branches. Since the clusters present different levels of background contamination (from G 219, where it is almost inexistent, up to G 108, which is strongly contaminated) and different degrees of concentration, the definition of the “best annulus” varies from cluster to cluster.

We list in Table 2 the ridge lines adopted for the various clusters. We note that, in general, the ridge line traced using the more internal annuli yields slightly bluer colors (by ~ 0.01 mag) at fixed luminosity. This may be due to residual field contamination in the more external areas, to blending effects (along the RGB, brighter stars are redder than fainter ones, and the blend is

slightly brighter and bluer than the original bright component) or to a true color gradient across the cluster. Since we do not have any suitable tool to disentangle these aspects, we have made our own best choice, which may be uncertain to ± 0.02 mag at least. Moreover, due to statistical reasons, it is quite difficult to firmly trace the brightest part of the giant branch as only few very bright stars actually populate the different annuli.

3.3. Adopted reddenings and metallicities

Estimates of reddening and metallicity for the program clusters are already available in the literature or can be derived from available data. The simplest and most straightforward procedure is then to adopt these values, which are independent of the *HST* observations.

Table 1, col. 10 reports the estimates of the reddening $-E(B-V)-$ we made from the HI maps (Burstein and Heiles 1982, Figure 4g). They are substantially identical to the values reported by Ajhar et al. (1996) and Rich et al. (1995), based on the same procedure. Though alternative estimates can be derived (see below), we have adopted these values for $E(B-V)$ in the calculation of the luminosity-metallicity calibration.

Concerning metallicity we note that, while it has been impossible so far to get CMDs from ground-based observations of the M31 GCs, several estimates of their metallicities could be obtained from spectroscopy and multi-color photometry of the cluster integrated light (see Huchra et al. (1991), Bonoli et al. (1987) for further references).

We report in Table 1 (col. 7, 9) the values of $[Fe/H]$ for the program clusters obtained by Huchra et al. (1991) from a set of spectroscopic indices, and those reported by Bonoli et al. (1987) from V-K integrated colors calibrated in terms of $[Fe/H]$. These two estimates are totally independent and their major difference is that the former are reddening independent, while the latter require the knowledge of the individual reddenings. Apart from the quality of the observational data, another source of error and/or systematic differences is also due to the different calibrations in terms of $[Fe/H]$ of the adopted indicators. In col. 8, we report the value of the metallicity obtained from the same original V-K data but using a revised calibration (Federici et al. 1996, in preparation). In general, all these estimates are in sufficiently good agreement for most clusters, although some more information seems to be essential in a few cases. In particular for G280 the photometric and spectroscopic metallicities are significantly different, while the revised calibration of the V-K data yields an intermediate value, which has then been adopted.

On the other hand, the availability of new, sufficiently reliable ridge lines for the giant branches allows for the first time to estimate the metallicity also by comparing the morphology and slope of the RGB of each individual M31 GC with a reference grid of Galactic GCs with known metallicities in the same observational plane (see for instance Da Costa and Armandroff (1990), who applied this procedure to 6 globular clusters in the Galaxy). As already done by Ajhar et al. (1996) and further discussed in Sect. 3.4, the direct comparison of the morphology of the RGB

(made by searching for the best match of the the ridge lines, independent of any constraints on reddening and distance) can yield very useful indication on the cluster metal content, for instance by considering the slope and degree of bending of the giant branch.

This comparison essentially confirms for all the clusters the reliability of the adopted values and the ranking, except maybe for G1 (see Sect. 3.4). However the *absolute* location of the RGB in the ($M_V, B-V$) plane (or equivalent) depends also on the reddening and distance of the cluster, and disentangling the effects of these parameters is not a trivial task, especially when the observational errors are still rather large. We have therefore decided to adopt for the metallicities the values reported in Table 3, col. 4, and use the comparison with a reference grid of Milky Way globulars just as a qualitative check (see Sect. 3.4).

Alternative procedures are also feasible, though less straightforward and accurate, which for instance may be useful for Bo468, never observed so far to get metallicity estimates. In particular, one could apply the method developed by Sarajedini (1994, hereafter *S-M*). This method would in principle allow to determine $[Fe/H]$ and $E(V-I)$ simultaneously from the giant branch. However, as noted by Ajhar et al. (1996), higher precision photometry than provided by the current data is really needed for this method. Nonetheless, the use of this procedure yields estimates fully consistent within the errors with the adopted values for all considered clusters. In particular, for Bo468, the value of metallicity reported in Table 3 (col. 4) has been obtained by adopting $E(B-V)=0.06$ from the HI maps and then using the *S-M* to get $[Fe/H]$. Note that without any assumption on $E(B-V)$, the *S-M* would converge for Bo468 to $E(B-V)= 0.07 \pm 0.04$ and $[Fe/H] = -0.61 \pm 0.40$.

3.4. A reference grid: comparison with the Milky Way globulars

As explained above, the comparison of the morphological shapes of the RGBs with a grid of reference clusters of known metallicities can be used as a further “quality check” of the adopted $[Fe/H]$, or to get useful indication in those cases where the spectroscopic and photometric determinations disagree significantly (e.g. G280) or are missing altogether.

In this procedure the weakest points are the lack of precise measures of individual reddening, that can be known only roughly with an error hardly smaller than about 0.03 mag, and the impossibility to account for some distance dispersion, which would be about ± 0.05 mag if the space distributions of the clusters is ~ 20 Kpc. Note that, assuming $A_V = 3.2E(B-V)$, the above uncertainties produce a “vertical” error of about 0.10 mag in addition to the observational error of the HB itself (see Table 3 and Sect. 4).

Adopting the values of reddening and metallicity reported in Table 3 (col.s 3, 4), and on the assumption that all M31 clusters are at the same distance (with adopted distance modulus to M31 $(m-M)_o = 24.43$, Freedman and Madore 1990), one can shift the RGB ridge lines in color and magnitude according to the adopted absorption law ($E(V-I)=1.342(B-V)$, $A_I = 1.858E(B-V)$, see

for reference Ajhar et al. (1996)) to get the *absolute* location of each individual cluster ridge line with respect to the reference grid based on the Milky Way globulars.

We present in Figure 5 the results we have obtained in the $(V,V-I)_o$ -plane for the 6 clusters observed with the WFPC2, and in Figure 6 those obtained in the $(B,B-V)_o$ -plane for the 2 clusters observed with the FOC. For summary and clarity, Table 4 reports the values of the various parameters eventually adopted for the M31 clusters and those for the Galactic reference clusters, whose data-base is briefly discussed below.

To ensure homogeneity with Da Costa and Armandroff (1990), we have adopted the relation $M_V^{HB} = 0.17 [\text{Fe}/\text{H}] + 0.82$ to set the distance-scale zero-point and dependence on $[\text{Fe}/\text{H}]$ of the "standard candle" (M_V^{HB}). In the $(V,V-I)_o$ -plane the Galactic data are taken from Da Costa and Armandroff (1990), (Table X), to which we added the $(V,V-I)_o$ data of NGC 6528 from Ortolani *et al.* (1992) and Guarnieri (1996, private communication). In the $(B,B-V)_o$ -plane we reported the ridge lines of M92 (Buonanno et al. 1985, Stetson and Harris 1988), M3 (Buonanno et al. 1994), 47 Tuc (Hesser et al. 1987), and NGC 6553 (Ortolani et al. 1995, Lanteri-Cravet, 1996, private communication) appropriately scaled by adopting the distance scale from Da Costa and Armandroff (1990), and the metallicity scale from Zinn (1985) and Armandroff (1989). As one can see from the Figures 5 and 6, the global matching is sufficiently good in both planes. This implies that the basic properties of the M31 clusters closely resemble those of the Galactic globulars of similar metal content. Of course, the agreement with the reference grid in the M_V^{HB} vs. color plane depends quite strongly also on the M_V^{HB} vs. $[\text{Fe}/\text{H}]$ relation assumed to derive the M_V^{HB} values for the reference Galactic clusters. Furthermore, small residual discrepancies can be ascribed to errors in the definition of the ridge lines and in the unknown distance dispersion of the GCs within M31. One notable exception seems to be the cluster G1, whose photometric and spectroscopic indices indicate a somewhat lower metallicity than suggested by its morphology in the $I_o, (V-I)_o$ plane (see Figure 5), which is similar to 47 Tuc. On the basis of this comparison alone, one could conclude that the metallicity of G1 is $[\text{Fe}/\text{H}] \sim -0.7$ (Rich *et al.* 1995). Since we decided to use this morphological comparison only as a quality check of metallicity, we have adopted the lower spectroscopic value of metallicity, $[\text{Fe}/\text{H}] = -1.08$ for consistency with the criteria we have applied on all the other clusters. However, we must keep in mind this discrepancy, and we shall see what impact it may have on our final luminosity-metallicity calibration (see Sect. 4).

3.5. The measure of the observed V_{HB}

Concerning specifically the measure of V_{HB} , we have adopted various approaches to take into account the intrinsic differences in the HB-morphologies, as done also by Ajhar et al. (1996). In particular, for the metal-poor clusters with sufficiently extended HBs (*i.e.* G219, G351, G105) we have computed a running mean over a 0.2 mag box moving along the HB in color, and we have adopted the value at $V-I \sim 0.5$, corresponding approximately to the center of the instability strip

(see Table 3, col. 5). The associated uncertainty is the observed *rms* vertical scatter of the HB at that color (see Table 3, col. 9).

For the metal rich objects, where the HB collapses to a red clump of stars, the identification of a reliable uncontaminated HB sample is extremely difficult. Besides applying the technique of the moving box adopted for the metal-poor clusters, we have also studied the Luminosity Function (LF) to locate the HB clump. The use of the LF is indeed made difficult by the fact that for metal-rich clusters the HB is also partially merging with the so-called RGB-bump (Thomas 1967), and the linear fit in Log of the RGB LF is actually broken in correspondence of the RGB-bump (Fusi Pecci et al. 1990). Due to this fact, the procedure of removing RGB stars from the LF as done by Ajhar et al. (1996) may be uncertain, though indicative. By coupling the two procedures we have eventually drawn the estimates reported in Table 3 (col. 5). The associated errors represent the observed *rms* scatter in the adopted box (see Table 3, col. 9).

A final general remark may be useful concerning the uncertainties affecting the adopted V_{HB} values. In fact, looking at the CMD's presented in Figure 4, one gets the impression that the HB is clearly visible for all the clusters in the top panel, while it is difficult to identify for instance for Bo 468 and G 280. Consequently, one might expect to find much larger errors in the measure of V_{HB} in the two latter cases. Actually, as shown in Table 8, column 9, the uncertainties we have determined for these clusters are slightly larger (0.04-0.05 mag) but not so much. This is essentially due to the ability of the procedures we adopted to locate fairly well the peak in the distributions in luminosity even if the color range of the HB is very narrow, giving the impression of a uniform clump of stars.

4. The M_V^{HB} vs. [Fe/H] calibration

Having determined the observed V_{HB} we can now consider the calibration of the standard candle. We adopt $(m-M)_o = 24.43$ (Freedman and Madore 1990) but other distance moduli spanning a range of at least ± 0.2 mag can be found in the literature (see for instance Pritchett & van den Bergh 1988, Christian & Heasley 1991). While this choice has no effect on the following discussion concerning the slope of the relation, it is crucial for the comparison of the zero-points and, in turn, for the problem of *absolute* ages. Note that an uncertainty of ~ 0.07 mag in the zero-point implies a corresponding uncertainty of ~ 1 Gyr in age.

Most of the impact on the determination of the slope comes from two basic items, *i.e.* the need for a correction of the observed V_{HB} to take into account the influence of the HB-morphology variations with varying metallicity, and the treatment of the *global* errors associated to the individual M_V^{HB} and [Fe/H] values adopted for each considered cluster. Note that, as explained below, the first item affects mostly the slope, while the second one essentially drives its associated error.

Concerning the first aspect, it is well known that metal-rich GCs in the Milky Way do not

contain any HB star a part from those populating a red stubby clump, which is however slightly brighter (by a quantity ΔV_{HB}^{rich}) than the average luminosity RR Lyrae variables would have, if they existed in these metal-rich clusters, according to stellar evolution theory (see for instance Lee et al. 1994). While the need for such a correction is generally accepted, its absolute size is a matter of discussion and it largely depends on theoretical models. Following Sarajedini et al. (1995), Ajhar et al. (1996) and Catelan & de Freitas Pacheco (1996), we have adopted a correction $\Delta V_{HB}^{rich} = 0.08\text{mag}$ to the values of the observed V_{HB} (Table 3, col. 5) for the clusters with $[\text{Fe}/\text{H}] > -1.0$ (see col. 7). This represents a compromise among possible values ranging from ~ 0.05 to 0.12 mag, as reported in the above quoted studies. According to the theoretical ZAHB models by Sweigart et al. 1987, Castellani et al. 1991 and Dorman 1992, a value around $0.09\text{-}0.10$ would be appropriate (see also Fullton et al. (1995), however we have adopted 0.08 for consistency with Ajhar et al. (1996).

In Sect. 3 we have discussed several possible error sources, which include contributions from: a) the adopted measure of V_{HB} (due to photometric errors, crowding, statistics, etc.); b) aperture photometry corrections and differences between the two cameras; c) the photometric transformations and the definition of the zero-points; d) the individual reddenings; e) the adopted reddening law; f) the metallicity estimates, etc. Moreover, we have assumed that the clusters are located at the same distance to us. The reliability of this assumption is actually the "intrinsic" strength of this procedure. However, this is not true in reality, and (small, i.e. $\leq \pm 0.05$ mag) differential distances also contribute to the scatter in the derived relation.

It is therefore quite hard to quantify precisely a fair measure of the *global* error one should associate to each individual value while combining all the available data to yield a final M_V^{HB} vs. $[\text{Fe}/\text{H}]$ calibration.

To reach a conclusion (at least provisional, until new information will become available) we have decided to add in quadrature to each formal error obtained from the procedures described at Sect. 3.5 (see Table 3, col. 9) an additional error of 0.10 mag which should statistically include the effects of all the above mentioned sources of uncertainty, allowing also for the fact that some of them could compensate each other to some extent. The final figures so obtained and adopted for the *global* error (as 1σ error-bar) are listed in Table 3, col. 10.

In Figure 7 we show the best linear fit obtained by taking into account the size of the errors on both variables simultaneously, and the two ($\pm 1\sigma$) solutions of the slope coefficient, normalized at $[\text{Fe}/\text{H}] = -1.1$. The final M_V^{HB} vs. $[\text{Fe}/\text{H}]$ relation so obtained is:

$$M_V^{HB} = (0.13 \pm 0.07) [Fe/H] + (0.95 \pm 0.09)$$

This result is of course strongly dependent on the various assumptions (more or less explicitly) made during the whole procedure, and should be used with care. The following considerations may thus be useful:

1. The *zero-point* is totally dependent on the adopted distance modulus to M31 and, moreover, it depends on the zero-points of the *HST* photometric calibrations (which are uncertain to $\sim \pm 0.05$ mag). As already pointed out, this aspect is crucial to any use of this relation to get distances and *absolute* ages of globular clusters, and we recall that a variation of $\sim +0.07$ mag implies an age increase of $\sim +1$ Gyr.
2. The *slope* and its accuracy depend on several different aspects, which can be schematically summarized as: (a) systematic differential errors in the zero-points of the various camera configurations; (b) systematic differential errors in the measurement of V_{HB} with varying HB morphology, like for instance the correction for the red HBs. If this correction were assumed to be ~ 0.10 mag the slope of this relation would become 0.15 ± 0.07 ; (c) errors in the metallicity estimates. In this respect, assuming for instance for G1 $[\text{Fe}/\text{H}] = -0.70$ rather than -1.08 (see Sect. 3.4), the slope of the relation would be 0.12 ± 0.07 ; (d) distance dispersion within M31. If one wanted to be extremely conservative, one could adopt an error of ± 0.15 mag for V_{HB} for all clusters, and one would then obtain:

$$M_V^{HB} = (0.13 \pm 0.10) [Fe/H] + (0.95 \pm 0.12)$$

To have further insights on the intrinsic reliability of the M_V^{HB} vs. $[\text{Fe}/\text{H}]$ relation here obtained, it could also be useful to examine homogeneous subsamples of clusters obtained with the same camera setup. In particular, one would get the following relations:

$$M_V^{HB} = (0.07 \pm 0.10) [Fe/H] + (0.86 \pm 0.11)$$

from the 6 GCs observed with the WFPC2, irrespective of the camera operating temperature;

$$M_V^{HB} = (0.07 \pm 0.10) [Fe/H] + (0.87 \pm 0.12)$$

from the 5 GCs observed with the WFPC2 at constant temperature (-88°C); and

$$M_V^{HB} = (0.21 \pm 0.11) [Fe/H] + (1.11 \pm 0.14)$$

from the 2 GCs observed with the FOC. It is difficult to give more weight to the individual sub-sets than to the whole sample as the number of observed clusters is too low in all cases. However, considering the various results, it seems quite reasonable to conclude that the slope of the M_V^{HB} vs. $[\text{Fe}/\text{H}]$ relation one can deduce at this stage from the analysis of the M31 GCs is probably closer to 0.15, the value predicted by theoretical models (Sweigart et al. 1987, Lee et al. 1994) and by several studies using ground-based observations (see for references Lee et al. 1994), than to ~ 0.30 (or even larger) that was obtained from other methods (Sandage 1982, 1993). In this respect, a final comment may be worth of note. The use of the de-reddened V_{HB} values without adopting any correction for the HB-morphology dependence (*i.e.* assuming $\Delta V_{HB}^{rich} = 0.00$) would yield over the whole sample:

$$M_V^{HB} = (0.06 \pm 0.07) [Fe/H] + (0.84 \pm 0.09)$$

Although there is no doubt that the HB-morphology correction is needed, this confirms that the available data hardly support values as high as 0.30 or more for the slope of the M_V^{HB} vs. $[\text{Fe}/\text{H}]$ relation.

5. Conclusions and future prospects

The study of the M_V^{HB} vs. $[\text{Fe}/\text{H}]$ relation carried out using the first available data on the observations of M31 GCs with both imaging cameras of *HST* leads to conclude that there is no evidence of any significant discrepancy between the observational result and the HB-model predictions.

A wider sample of observed GCs in M31 is needed in order to reduce significantly the errors and confirm unambiguously the value of the slope derived in the present study, i.e. ~ 0.13 .

In particular, it would be very important to have data for clusters displaying a well populated HB, over a wide color range and covering an appropriate range in metallicity. A proposal by our team (GO 6671, P.I. M. Rich) has been granted *HST* time to observe 10 more GCs in M31 during Cycle 6. As soon as these new data will be available, we are confident that the long-standing issue of measuring the slope of the M_V^{HB} vs. $[\text{Fe}/\text{H}]$ relation will be settled.

It is a pleasure to thank our collaborators P. Battistini, F. Bonoli, I.R. King, and R. Walterbos for their contributions to this project. This research was supported by the *Consiglio delle Ricerche Astronomiche* (CRA) of the *Ministero delle Università e della Ricerca Scientifica e Tecnologica* (MURST), Italy, by the *Agenzia Spaziale Italiana* (ASI), and by the National Aeronautics and Space Administration, and the National Science Foundation, USA.

REFERENCES

- Armandroff, T.E. 1989, *AJ*, 97, 375
- Ajhar, E.A., Grillmair, C.J., Lauer, T.R., Baum, W.A., Faber, S.M., Holtzman, J.A., Light, R.M., Lynds, R., and O’Neil, Jr., E.J. 1996, *AJ*, 111, 1106
- Battistini, P., Bònoli, F., Braccesi, A., Federici, L., Fusi Pecci, F., Marano, B., and Borngen, F. 1987, *A&AS*, 67, 447
- Battistini, P.L., Bònoli, F., Casavecchia, M., Ciotti, L., Federici, L., and Fusi Pecci, F. 1993, *A&A*, 272, 77
- Bendinelli, O., Cacciari, C., Djorgovski, S., Federici, L., Ferraro, F.R., Fusi Pecci, F., Parmeggiani, G., Weir, N., and Zavatti, F. 1993, *ApJ*, 409, L17

- Bica, E., Barbuy, B., and Ortolani, S. 1991, *ApJ*, 382, L15
- Bolte, M., and Hogan, C.J. 1995, *Nature*, 376, 399
- Bònoli, F., Delpino, F.E., Federici, L., and Fusi Pecci, F. 1987, *A&A*, 185, 25
- Brodie, J.P. 1993, in: Smith G., Brodie J.P. (eds.) *The Globular Cluster – Galaxy Connection*, ASP Conf. Ser., 48, p.483
- Brodie, J.P., and Huchra, J.P. 1990, *ApJ*, 362, 503
- Buonanno, R., Buscema, G., Corsi, C.E., Ferraro I., and Iannicola G. 1983, *A&A*, 126, 278
- Buonanno, R., Corsi, C. E., and Fusi Pecci, F. 1985, *A&A*, 145, 97
- Buonanno, R., Corsi, C. E., and Fusi Pecci, F. 1989, *A&A*, 216, 80
- Buonanno, R., Corsi, C. E., Buzzoni, A., Cacciari, C., Ferraro, F.R., and Fusi Pecci, F. 1994, *A&A*, 290, 69
- Buonanno, R., Corsi, C.E., Pulone, L., Fusi Pecci, F., and Bellazzini, M., 1996, *AJ*, submitted
- Burstein, D. and Heiles, C. 1982, *AJ*, 87, 1165
- Castellani, V., Chieffi, A., and Pulone, L., 1991, *ApJS*, 76, 911
- Catelan, M., and de Freitas Pacheco, J.A. 1996, *PASP*, 108, 166
- Chaboyer, B., Demarque, P., and Sarajedini, A. 1996, *ApJ*, 459, 558
- Christian, C. A., and Heasley, J. N. 1991, *AJ*, 101, 848
- Cool, A. M. and King, I. R. 1995, in *Proc. of a STScI Workshop, Calibrating Hubble Space Telescope: Post Servicing Mission*, A. Koratkar and C. Leitherer (eds.), Baltimore, STScI, p. 290
- Couture J., Racine, R., Harris, W. E. and Holland, S. 1995, *AJ*, 109, 2050
- Da Costa, G.S., and Armandroff, T.E. 1990, *AJ*, 100, 162
- Dorman, B., 1992, *ApJS*, 81, 221
- Ferraro, F.R., Clementini, G., Fusi Pecci, F., and Buonanno, R. 1991, *MNRAS*, 252, 357
- Freedman, W.F., and Madore, B.F. 1990, *ApJ*, 365, 186
- Fullton, L.K., Carney, B.W., Olszewski, E.W., Zinn, R.J., Demarque, P., Janes, K.A., Da Costa, G.S., and Seitzer, P. 1995, *AJ*, 110, 652
- Fusi Pecci, F., Ferraro, F.R., Crocker, D.A., Rood, R.T., and Buonanno, R. 1990, *A&A*, 238, 95

- Fusi Pecci, F. Cacciari, C., Federici, L., and Pasquali, A. 1993, in: Smith G., Brodie J.P. (eds.) The Globular Cluster – Galaxy Connection, ASP Conf. Ser. No. 48, p.410
- Fusi Pecci, F., Battistini, P., Bendinelli, O., Bonoli, F., Cacciari, C., Djorgovski, S.G., Federici, L., Ferraro, F.R., Parmeggiani, P., Weir, N., and Zavatti, F. 1994, A&A, 284, 349
- Heasley J. N., Christian, C. A., Friel, E. D. and Janes, K. A. 1988, AJ, 96, 1312
- Hesser, J.E., Harris, W.E., Vandenberg, D.A., Allwright, J.W.B., Shott, P., and Stetson, P.B. 1987, PASP, 99, 739
- Holtzman, J. A., Burrows, C. J., Casertano, S., Hester, J. J., Trauger, J. T., Watson, A. M., and Worthey, G. 1995, PASP, 107, 1065
- Huchra J.P. 1993, in: Smith G., Brodie J.P. (eds.) The Globular Cluster – Galaxy Connection, ASP Conf. Ser., 48, p.420
- Huchra, J. P., Brodie, J. P. and Kent, 1991, ApJ, 370, 495
- Kurucz, R.L. 1979, ApJS, 40, 1
- Jedrzejewski, R.I., Hartig, G., Jakobsen, P., Crocker, J.H., and Ford, H.C. 1994, ApJ, 435, L7
- Lee, Y.W., Demarque, P., and Zinn, R.J. 1994, ApJ, 423, 248
- Moffat, A.F.J. 1969, A&A, 3, 455
- Ortolani, S., Barbuy, B., and Bica, E. 1990, A&A, 236, 362
- Ortolani, S., Barbuy, B., and Bica, E. 1992, A&AS, 92, 441
- Ortolani, S., Renzini, A., Gilmozzi, R., Marconi, G., Barbuy, B., Bica, E., and Rich, M. 1995, Nature, 377, 701
- Pritchett, C.J., van den Bergh, S. 1988, ApJ, 331, 135
- Rich, R.M., Mighell, K.J., Freedman, W.L., and Neill, J.D. 1995, AJ, 111, 768
- Sandage, A. 1982, ApJ, 252, 553
- Sandage, A. 1993, AJ, 106, 703
- Sandage, A., and Cacciari, C. 1990, ApJ, 350, 645
- Sarajedini, A. 1994, AJ, 107, 618
- Sarajedini, A., Lee, Y.-W., and Lee, D. H. 1995, ApJ, 450, 712
- Sargent, W.L.W., Kowal, C.T., Hartwick, F.D.A., and van den Bergh, S. 1977, AJ, 82, 947

- Savage, B. D., and Mathis, J.S. 1979, *ARA&A*, 17, 73
- Stetson, P.B., and Harris, W.E. 1988, *AJ*, 96, 909
- Sweigart, A.V., Renzini, A., and Tornambè, A. 1987, *ApJ*, 312, 762
- Thomas, H.C. 1967, *Z. Astrophys.*, 67, 420
- Vetesnik, M. 1962, *BAC*, 13,180
- Walker 1992, *ApJ*, 390, L81
- Zinn, R.J. 1985, *ApJ*, 293, 424

Fig. 1.— FOC/96 image of the globular cluster G351 in M31. Filter F480LP, co-added frames, total exposure time 3800 sec.

Fig. 2.— Adopted empirical transformations from the HST magnitude system to the Johnson standard system for the FOC/96.

Fig. 3.— Comparison of the CMD's of the globular cluster G105 in M31, based on the same WFPC2 original data. (a) this paper, (b) Ajhar et al. 1996.

Fig. 4.— CMD's obtained from the HST observations for the considered sample of 8 globular clusters in M31. The diagrams are ordered with increasing metallicity $[\text{Fe}/\text{H}]$ (see labels).

Fig. 5.— Comparison of the observed giant branches of a sample of reference Galactic globular clusters (dashed lines) and the observed M31 globulars (full line) in the $I_0, (V-I)_0$ plane. The Galactic globulars are M15, $[\text{Fe}/\text{H}]=-2.17$, NGC 6397, $[\text{Fe}/\text{H}]=-1.91$, M2, $[\text{Fe}/\text{H}]=-1.58$, NGC 6752, $[\text{Fe}/\text{H}]=-1.54$, NGC 1851, $[\text{Fe}/\text{H}]=-1.29$, 47Tuc, $[\text{Fe}/\text{H}]=-0.71$, NGC 6528, $[\text{Fe}/\text{H}]=-0.14$, from blue to red.

Fig. 6.— Comparison of the observed giant branches of a sample of reference Galactic globular clusters (dashed lines) and the observed M31 globulars (full line) in the $V_0, (B-V)_0$ plane. The Galactic globulars are M92, $[\text{Fe}/\text{H}]=-2.24$, M3, $[\text{Fe}/\text{H}]=-1.65$, 47Tuc, $[\text{Fe}/\text{H}]=-0.71$, NGC 6553, $[\text{Fe}/\text{H}]=-0.20$, from blue to red.

Fig. 7.— The adopted $M_V(\text{HB})$ vs $[\text{Fe}/\text{H}]$ relation obtained from the HST observations of the considered sample of 8 GC's in M31. The associated uncertainties are ± 0.2 dex in $[\text{Fe}/\text{H}]$ and the *global* limiting errors reported in Table 3, col. 10 (see Sect. 3.5 and 4). The full line represents the weighted best fit $M_V(\text{HB}) = 0.13 [\text{Fe}/\text{H}] + 0.95$; the dashed lines (normalized at $[\text{Fe}/\text{H}]=-1.1$) indicate the uncertainty in the slope (0.13 ± 0.07).

Table 1. Relevant data for the 8 globular clusters observed in M31 with HST.

Bo ^a	G ^a	Vet ^a	V	(B-V)	R _{kpc} ^b	[Fe/H] _p ^c	[Fe/H] _{pr} ^d	[Fe/H] _s ^e	E(B-V) _{BH} ^f	E(B-V) _S ^g
	1	MII	13.70	0.86	34.16	-1.33	-1.14	-1.08	0.05	0.03
6	58	55	15.60	0.89	6.32	-0.51	-0.72	-0.57	0.10	0.11
343	105	199	16.35	0.69	14.52	-1.25	-1.11	-1.49	0.06	0.04
45	108	94	15.77	0.88	4.81	-0.86	-1.08	-0.94	0.12	...
358	219	MIV	15.11	0.60	19.53	-2.28	-1.90	-1.83	0.06	0.03
225	280	282	14.26	0.92	4.59	-0.21	-0.44	-0.70	0.09	...
405	351	140	15.16	0.72	17.71	-1.95	-1.82	-1.80	0.10	...
468			18.12	0.53	19.80	0.06	0.07

^aBo from Battistini et al. (1987), G from Sargent et al. (1977), Vet from Vetesnik (1962)

^badopting for M31 a distance of 770 kpc, corresponding to $(m - M)_0 = 24.43$

^cmetallicities from infrared colors $(V - K)_0$ (Bönoli et al. 1987)

^dmetallicities from $(V - K)_0$, using $E(B - V)_{BH}$ and the calibration from Brodie & Huchra (1990)(Federici et al. 1996, in preparation)

^emetallicities from spectral indices (Huchra et al. 1991)

^freddenings from the HI maps (Burstein & Heiles 1982)

^greddenings obtained applying the method developed by Sarajedini (1994)

Table 2. Ridge lines for the 8 globular clusters observed in M31 with HST.

G219		G351		G105		G1	
I	(V-I)	V	(B-V)	I	(V-I)	I	(V-I)
20.50	1.52	22.34	1.70	20.50	1.73	20.75	2.40
21.00	1.37	22.50	1.58	21.00	1.53	21.00	2.00
21.50	1.28	23.00	1.36	21.50	1.40	21.50	1.64
22.00	1.20	23.50	1.22	22.00	1.29	22.00	1.45
22.40	1.16	24.00	1.10	22.50	1.21	23.00	1.20
23.00	1.09	24.50	1.00	23.00	1.15	23.50	1.12
23.45	1.05	25.00	0.92	23.50	1.10	24.00	1.07
24.00	1.01	25.50	0.89	24.00	1.05	24.50	1.02
25.00	0.94	26.00	0.88	25.00	1.00	25.00	0.95

G108		Bo468		G58		G280	
I	(V-I)	I	(V-I)	I	(V-I)	V	(B-V)
20.75	2.20	21.00	2.00	21.00	3.00	25.00	2.40
21.00	1.90	21.30	1.80	21.50	2.00	24.50	2.17
21.50	1.68	21.75	1.60	21.65	1.80	24.00	1.90
22.00	1.54	22.45	1.40	22.00	1.65	23.55	1.68
22.50	1.43	23.60	1.20	22.50	1.50	23.50	1.64
23.00	1.35	24.00	1.15	23.00	1.35	23.55	1.60
23.30	1.30	24.40	1.10	23.50	1.27	24.00	1.45
24.00	1.20	24.95	1.05	24.00	1.20	24.50	1.33
24.45	1.17	25.30	1.00	24.52	1.17	25.00	1.26
25.00	1.13	25.80	0.95	25.00	1.15	25.50	1.20
...	26.00	1.10

Table 3. Adopted reddenings, metallicities and Horizontal Branch magnitudes

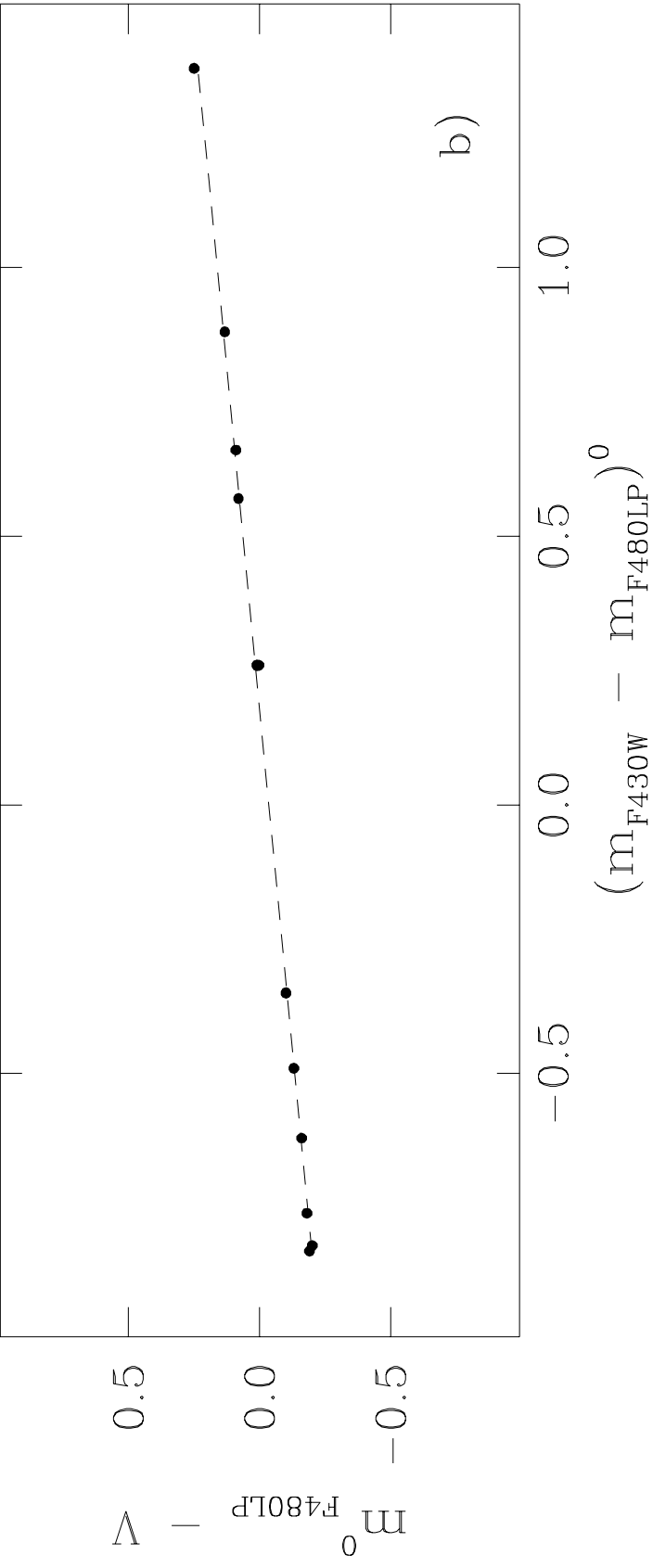
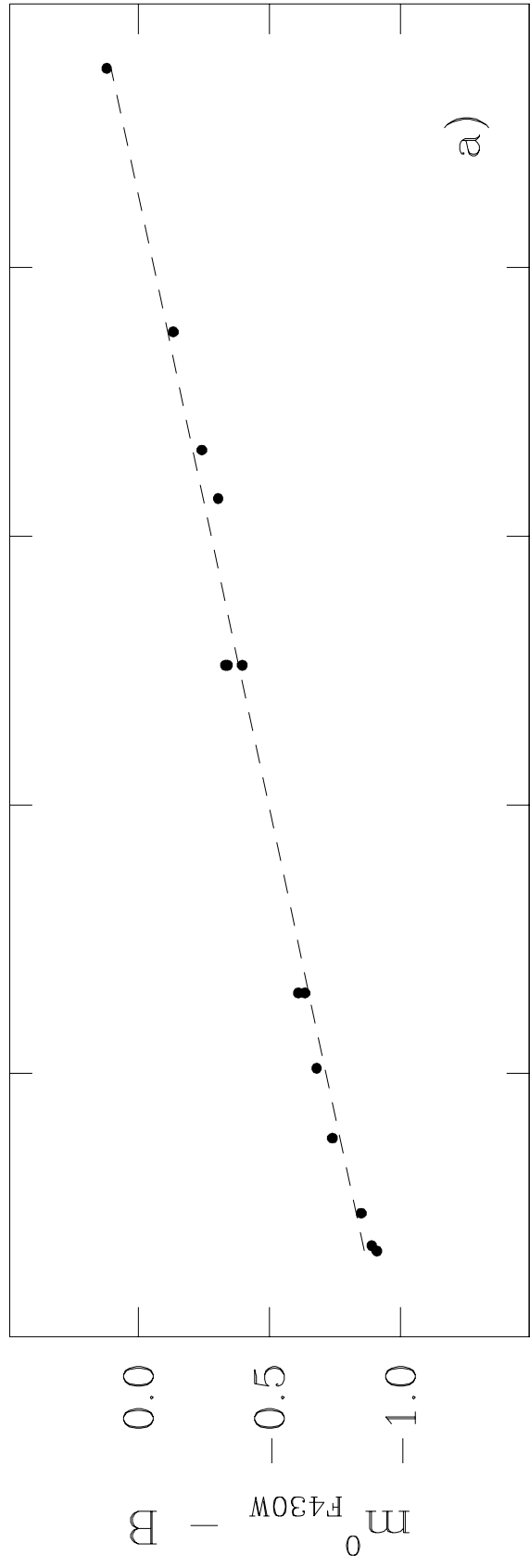
Bo	G	$E(B-V)_{ad}$	$[Fe/H]_{ad}$	V(HB)	$V_0(\text{HB})$	$V_0(\text{HB})^{cor}$	$M_V(\text{HB})_0^{cor}$	$\epsilon V(\text{HB})$	
								*	+
	1	0.05	-1.08	25.31	25.15	25.15	0.72	0.05	0.11
6	58	0.10	-0.57	25.45	25.13	25.21	0.78	0.03	0.10
343	105	0.06	-1.49	25.49	25.30	25.30	0.87	0.03	0.10
45	108	0.12	-0.94	25.53	25.15	25.23	0.80	0.03	0.10
358	219	0.06	-1.83	25.29	25.10	25.10	0.67	0.03	0.10
225	280	0.09	-0.40	25.66	25.37	25.45	1.02	0.04	0.11
405	351	0.10	-1.80	25.48	25.16	25.16	0.73	0.06	0.12
468		0.06	-0.61	25.40	25.21	25.29	0.86	0.05	0.11

*formal rms-scatter in the adopted HB box (see Sect. 3.5)

+global error (see Sect. 4)

Table 4. Adopted values for the MW.

Names	$[Fe/H]_{ad}$	$E(B - V)_{ad}$	$(m - M)_0$
M92	-2.24	0.02	14.46
M 15	-2.17	0.10	15.41
NGC 6397	-1.91	0.18	12.40
M3	-1.65	0.00	14.94
M 2	-1.58	0.02	15.50
NGC 6752	-1.54	0.04	13.19
NGC 1851	-1.29	0.02	15.45
47Tuc	-0.71	0.04	13.51
NGC 6528	-0.14	0.60	14.43
NGC 6553	-0.20	0.80	13.65



G105

